Supporting Information for

Perfectly isoselective polymerization of 2-vinylpyridine promoted by *β*-diketiminato rare-earth metal cationic complexes

Zehuai Mou*, Qingxiang Zhuang, Hongyan Xie, Yunjie Luo* and Dongmei Cui

Table of Contents

1. ^{1}H NMR and ^{13}C NMR spectra of complexes 1a-2b

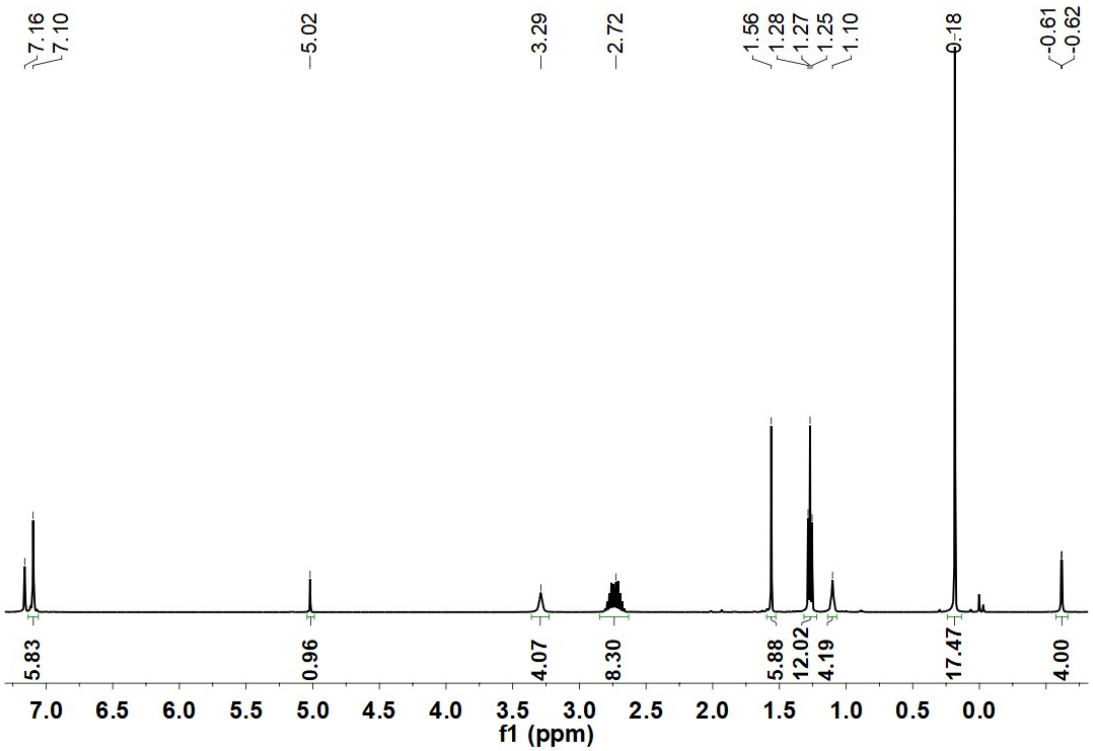

Fig. S1. ^{1}H NMR spectrum (C_6D_6, 500 MHz) of complex **1a**.

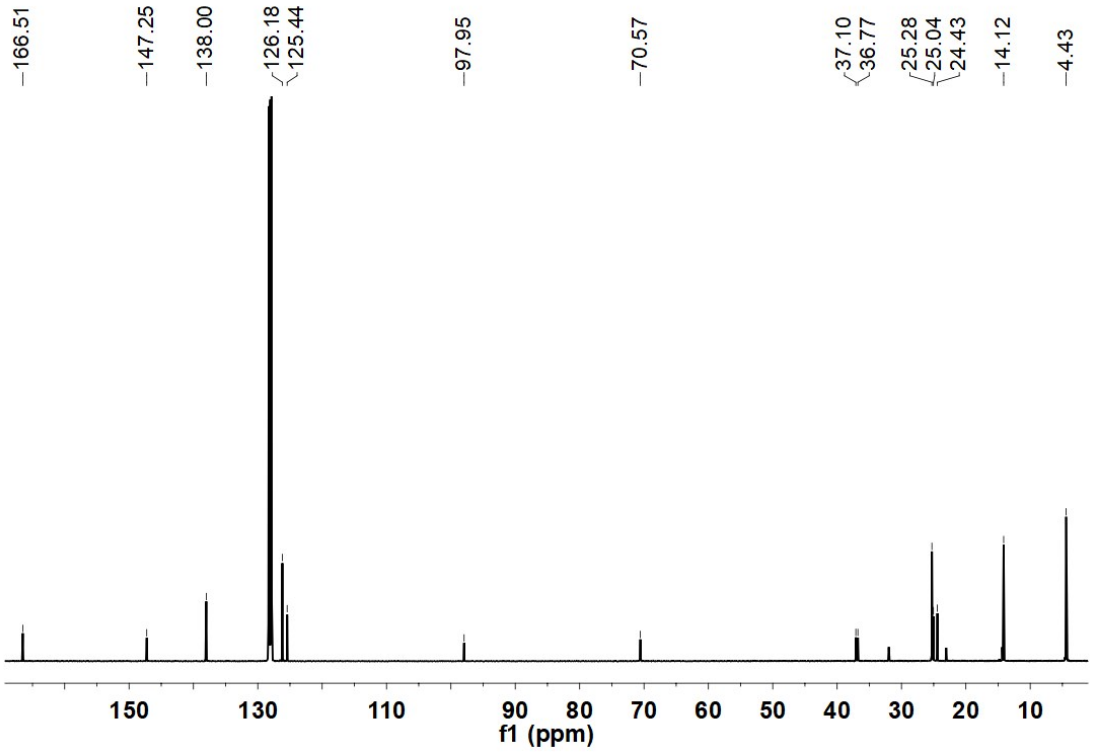

Fig. S2. ^{13}C NMR spectrum of (C_6D_6, 125 MHz) of complex **1a**.

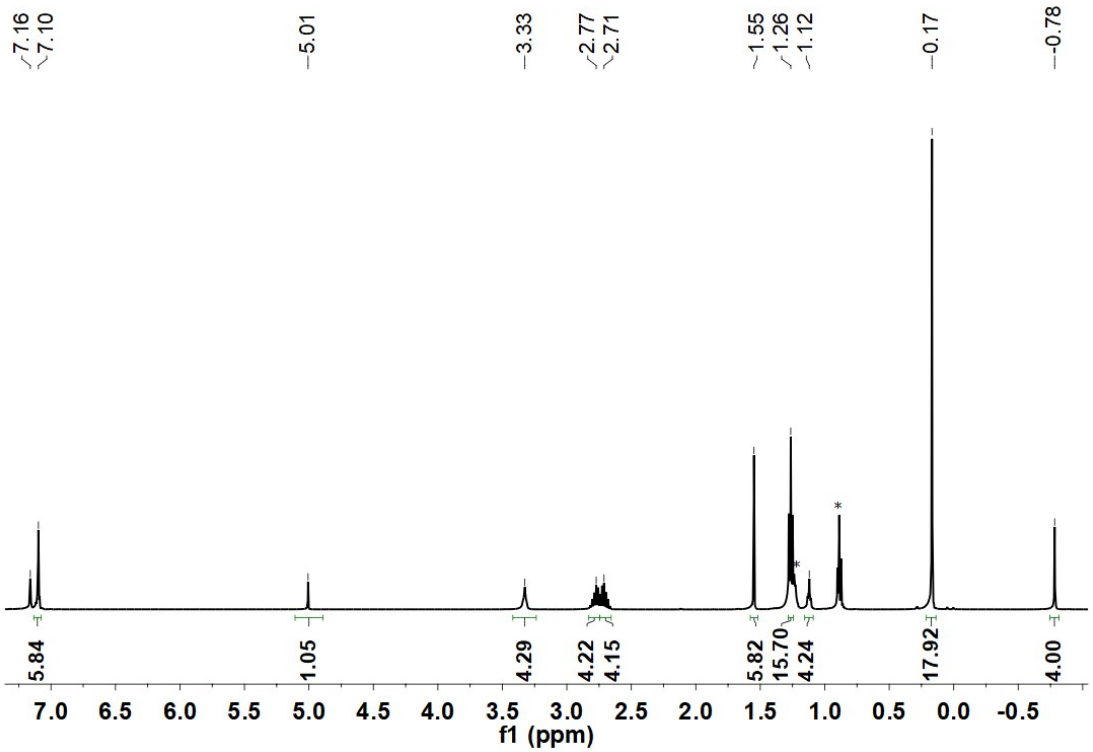

Fig. S3. ^{1}H NMR spectrum (C_6D_6, 500 MHz) of complex **1b**. (*: hexane)

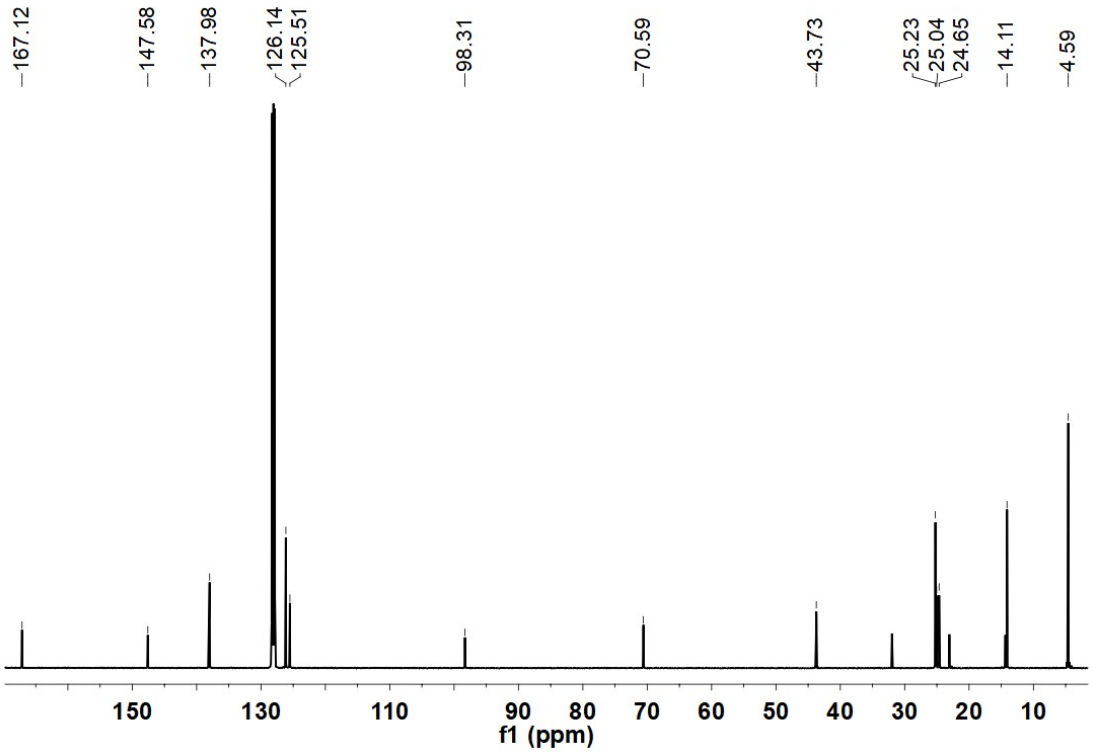

Fig. S4. ^{13}C NMR spectrum of (C_6D_6, 125 MHz) of complex **1b**.

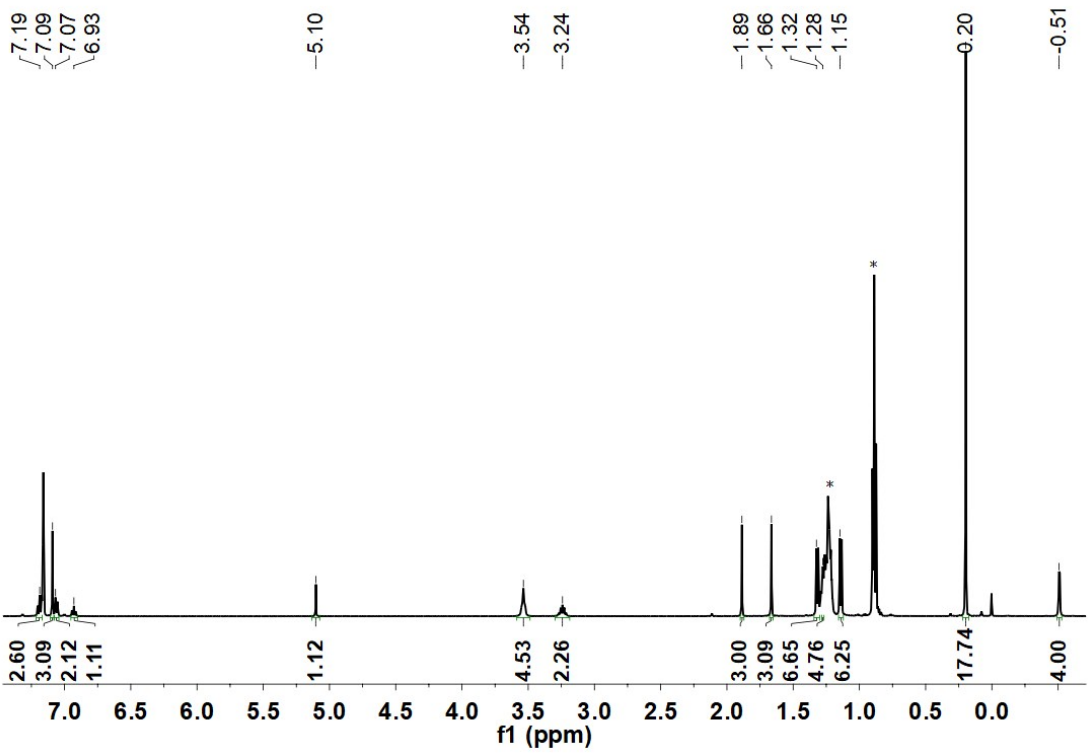

Fig. S5. ^{1}H NMR spectrum (C_6D_6, 500 MHz) of complex **2a**. (*: hexane)

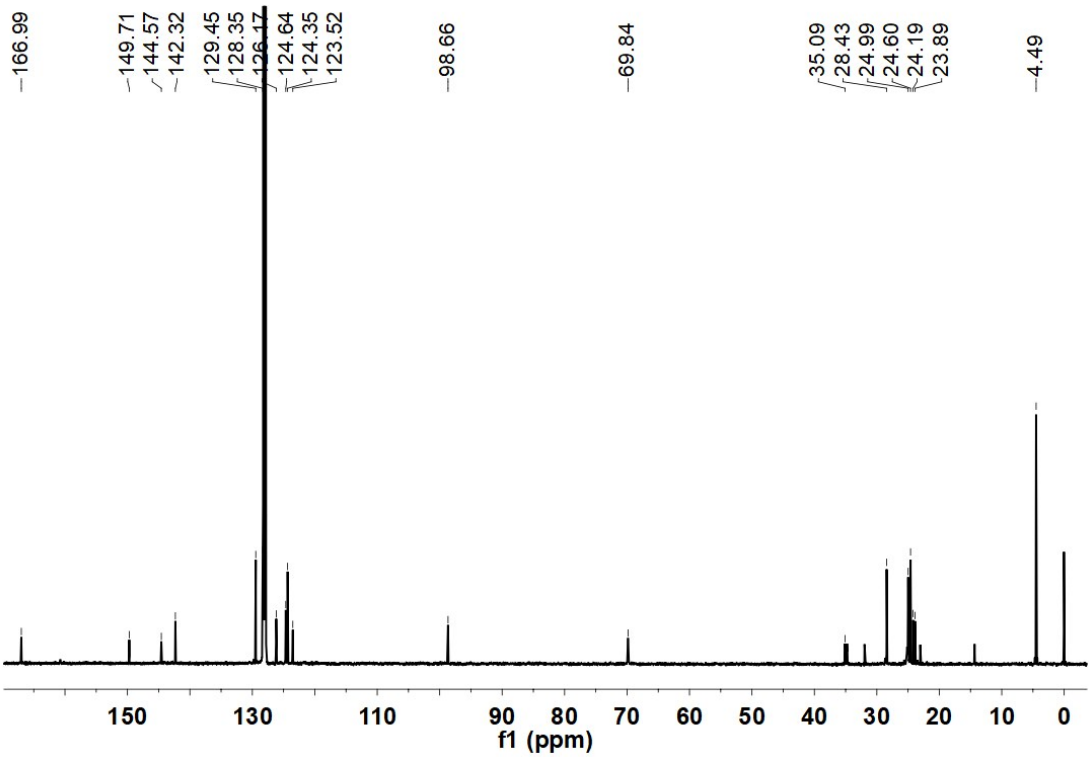

Fig. S6. ^{13}C NMR spectrum of (C_6D_6, 125 MHz) of complex **2a**.

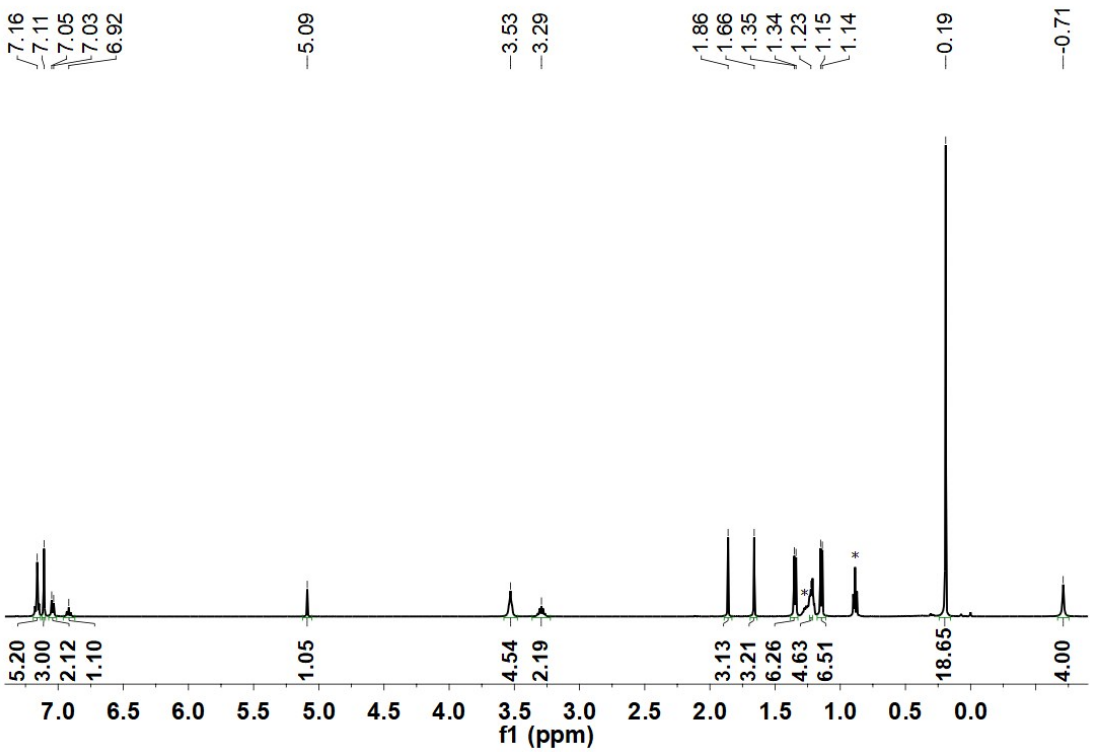

Fig. S7. ^{1}H NMR spectrum (C_6D_6, 500 MHz) of complex **2b**. (*: hexane)

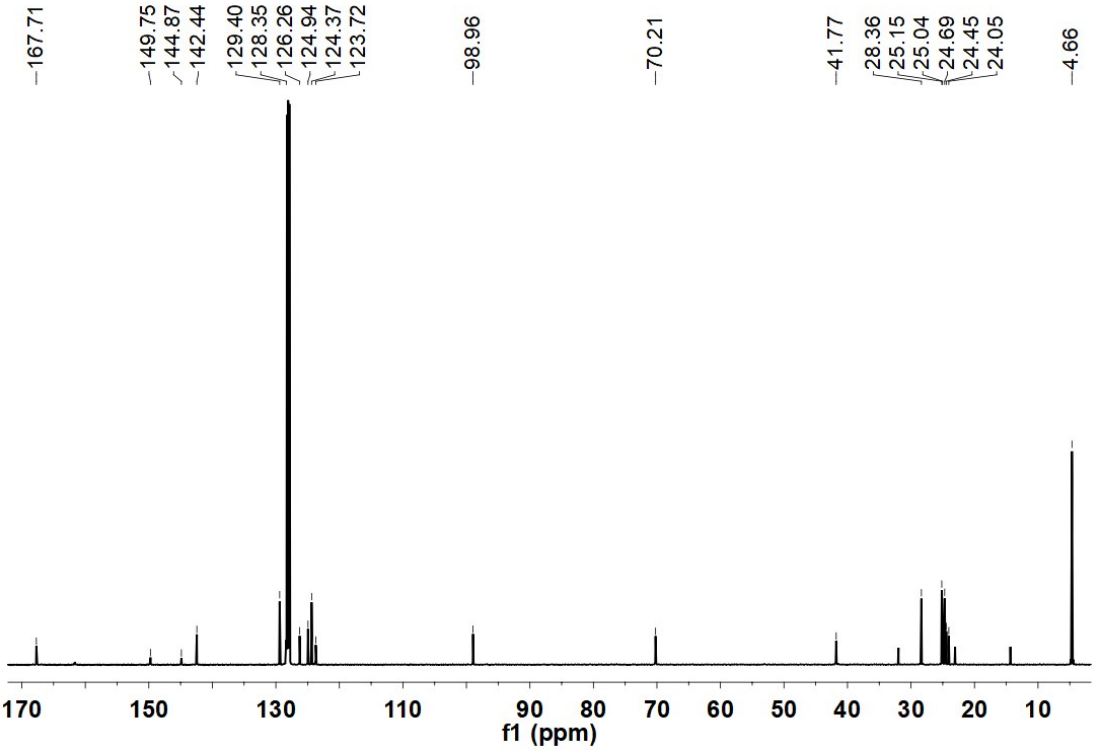

Fig. S8. ^{13}C NMR spectrum of (C_6D_6, 125 MHz) of complex **2b**.

2. Determination of isotacticity of resulting P2VP based on ^{13}C NMR spectroscopy

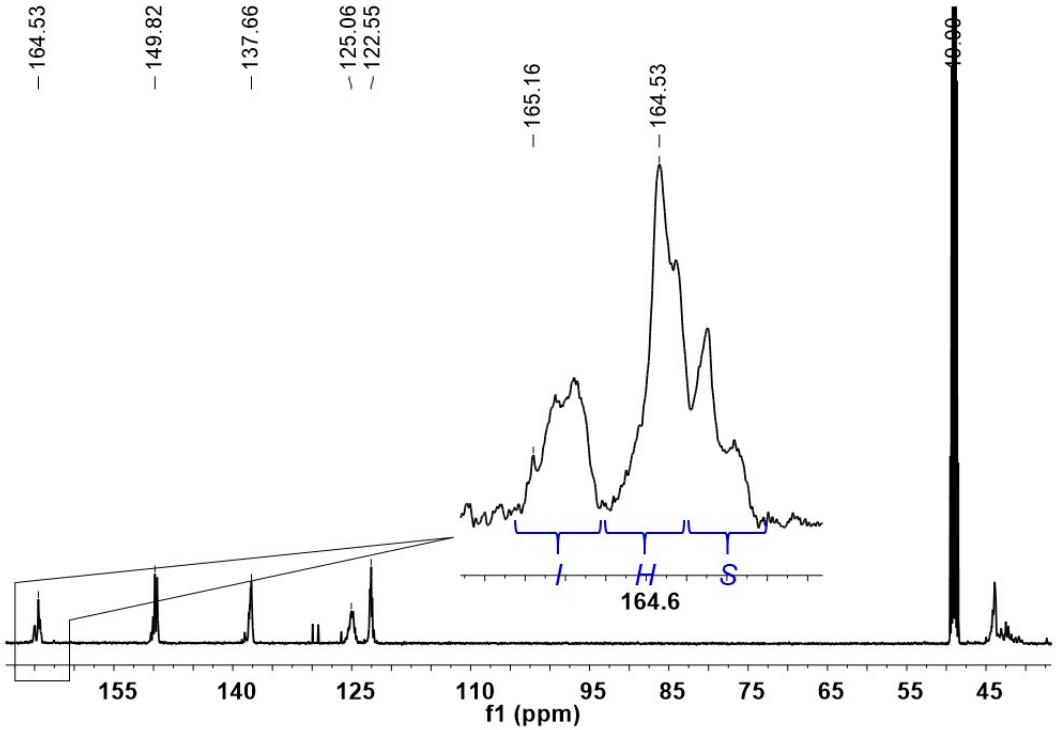

mm is isotactic triad made up of two adjacent *meso* diads, and determined with the integral of aromatic quaternary carbon in ^{13}C NMR spectrum (CD_3OD, 125 MHz) based on the following equation[1]:

$$mm = I/(I+H+S) \times 100\%$$

3. Representative ^{1}H NMR and ^{13}C NMR spectra of resulting P2VPs obtained under different conditions

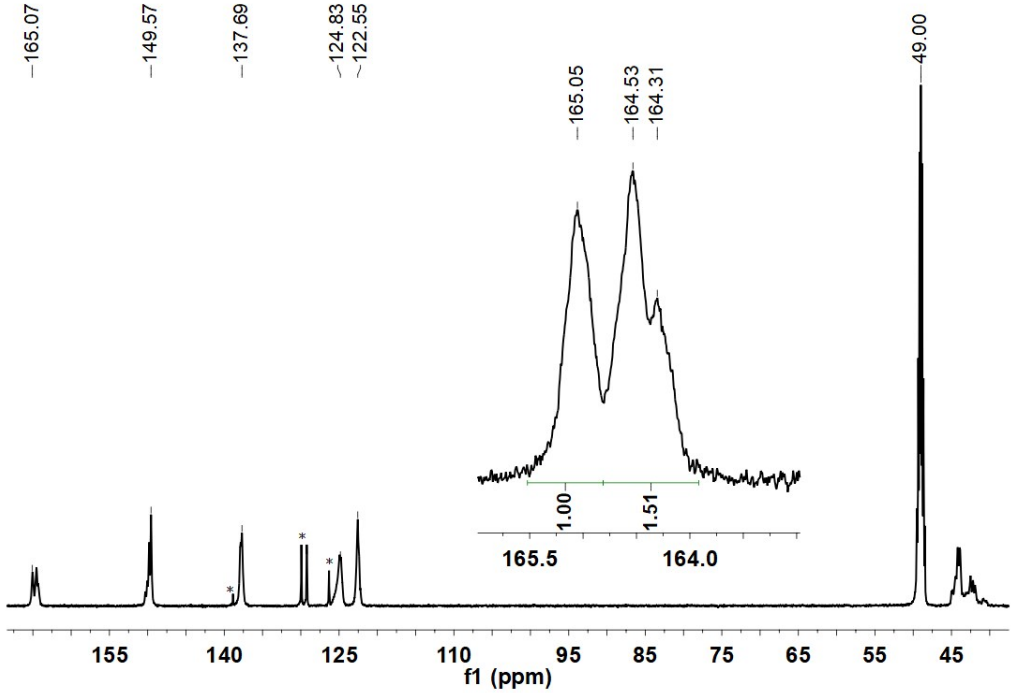

Fig. S9. ^{13}C NMR spectrum (CD_3OD, 125 MHz) of P2VP produced by complex **1a** in toluene. (mm = 40%, *: toluene)

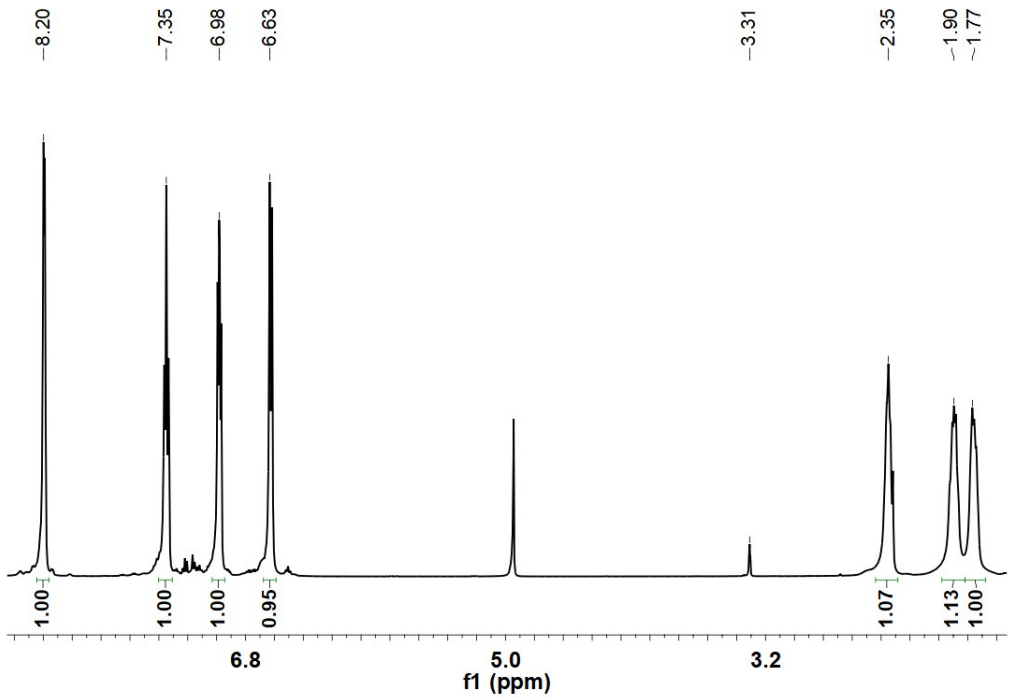

Fig. S10. ^{1}H NMR spectrum (CD_3OD, 500 MHz) of isotactic P2VP produced by **1a**/$[Ph_3C][B(C_6F_5)_4]$ in toluene.

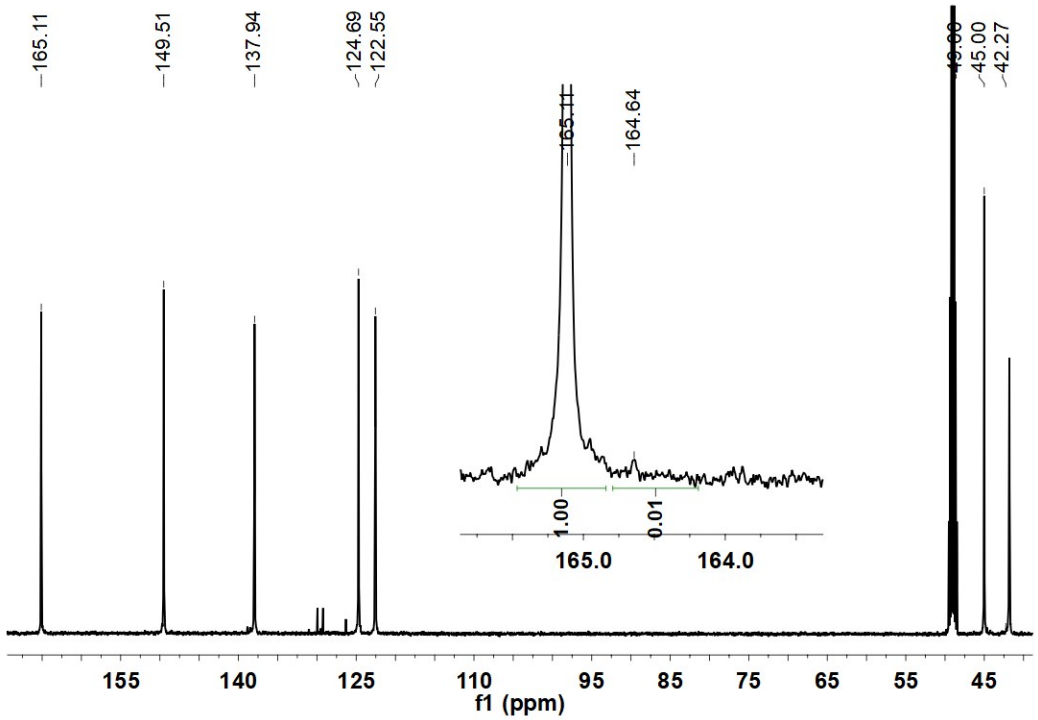

Fig. S11. ^{13}C NMR spectrum (CD_3OD, 125 MHz) of isotactic P2VP produced by **1a**/$[Ph_3C][B(C_6F_5)_4]$ in toluene. (mm = 99%)

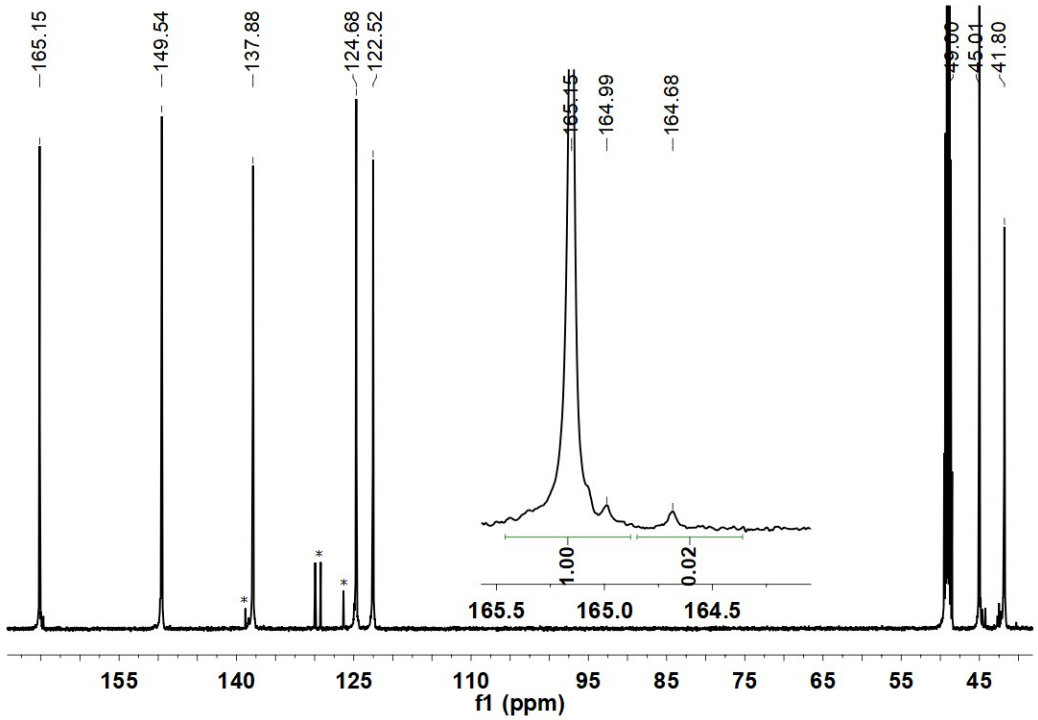

Fig. S12. ^{13}C NMR spectrum (CD_3OD, 125 MHz) of isotactic P2VP produced by **1b**/$[Ph_3C][B(C_6F_5)_4]$ in toluene. (mm = 98%, *: toluene)

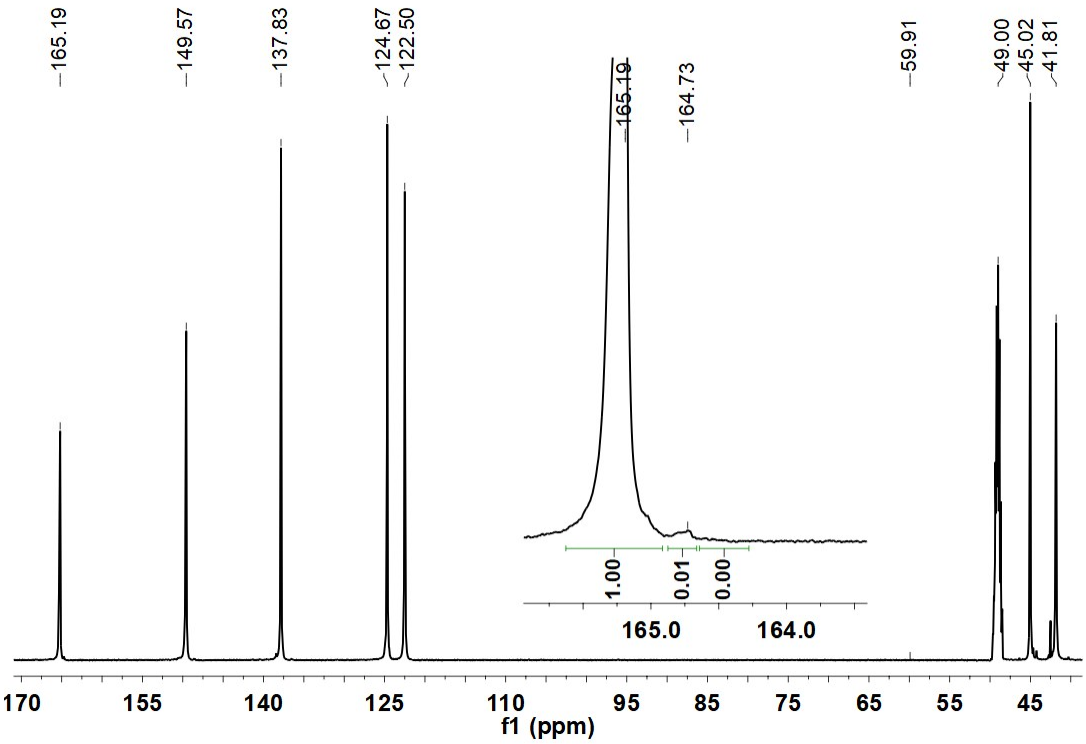

Fig. S13. ^{13}C NMR spectrum (CD_3OD, 125 MHz) of isotactic P(2-VP) produced by **1a**/$[Ph_3C][B(C_6F_5)_4]$ in toluene. (mm = 99%, 2-VP feed ratio: 500)

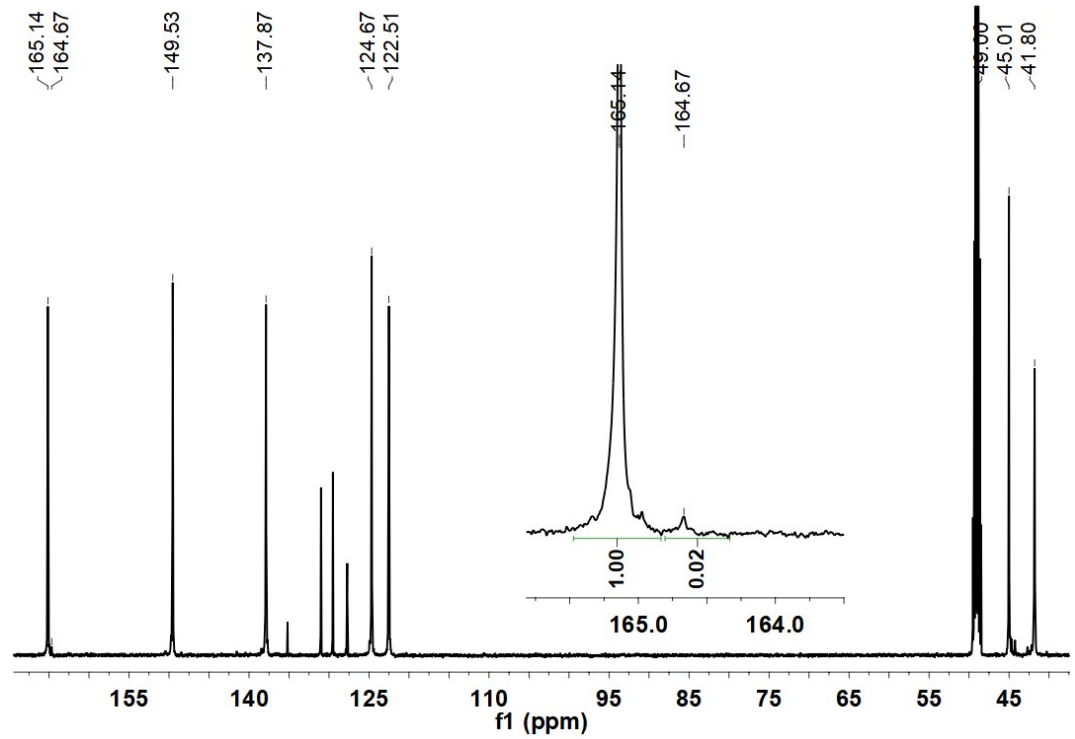

Fig. S14. ^{13}C NMR spectrum (CD_3OD, 125 MHz) of isotactic P(2-VP) produced by **1a**/$[Ph_3C][B(C_6F_5)_4]$ in PhCl. (mm = 98%)

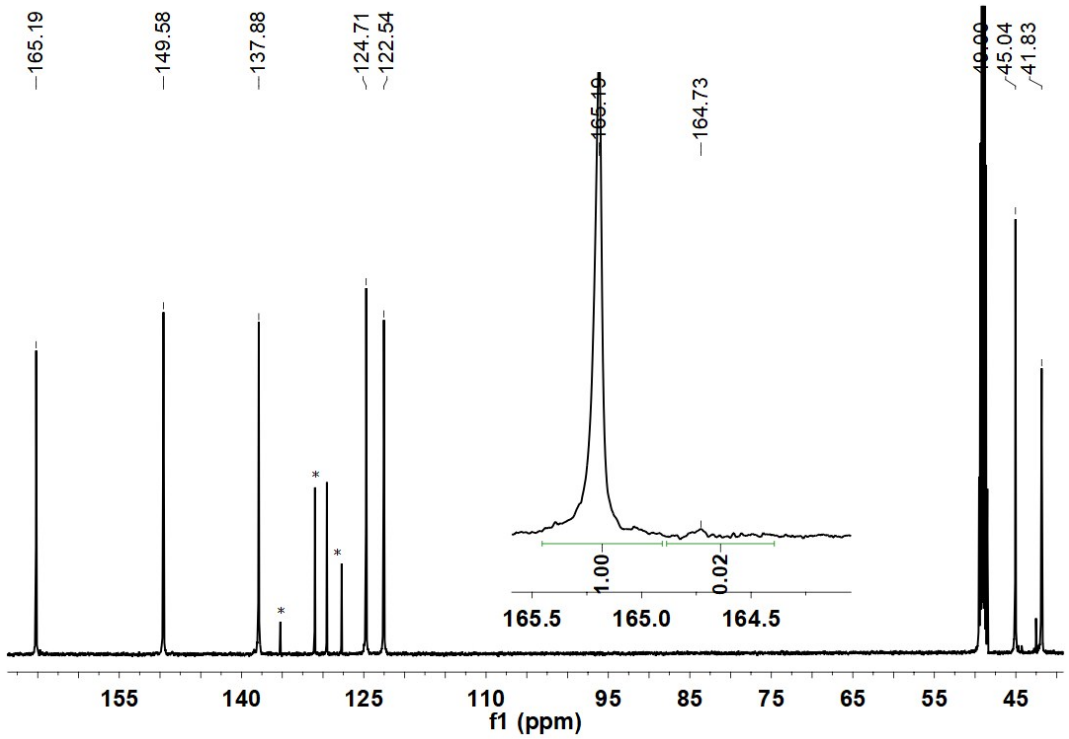

Fig. S15. ^{13}C NMR spectrum (CD_3OD, 125 MHz) of isotactic P2VP produced by **1a**/[$PhNHMe_2$][$B(C_6F_5)_4$] in PhCl. (mm = 98%, *: PhCl)

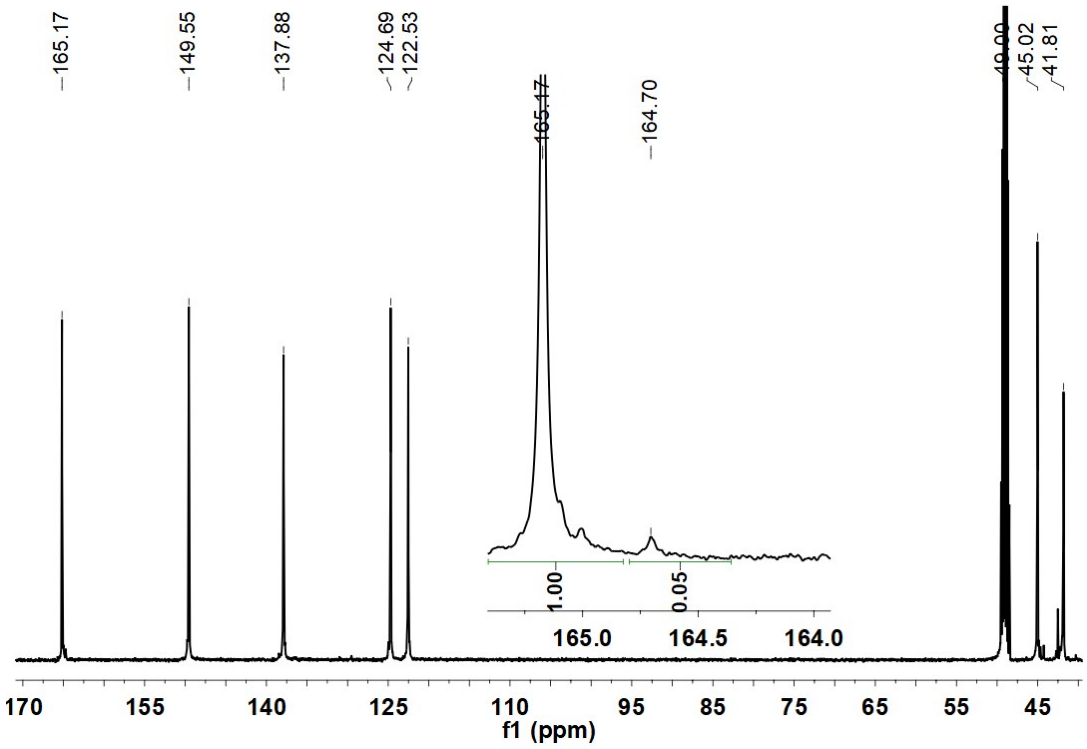

Fig. S16. ^{13}C NMR spectrum (CD_3OD, 125 MHz) of isotactic P2VP produced by **1b**/[$PhNHMe_2$][$B(C_6F_5)_4$] in PhCl. (mm = 95%)

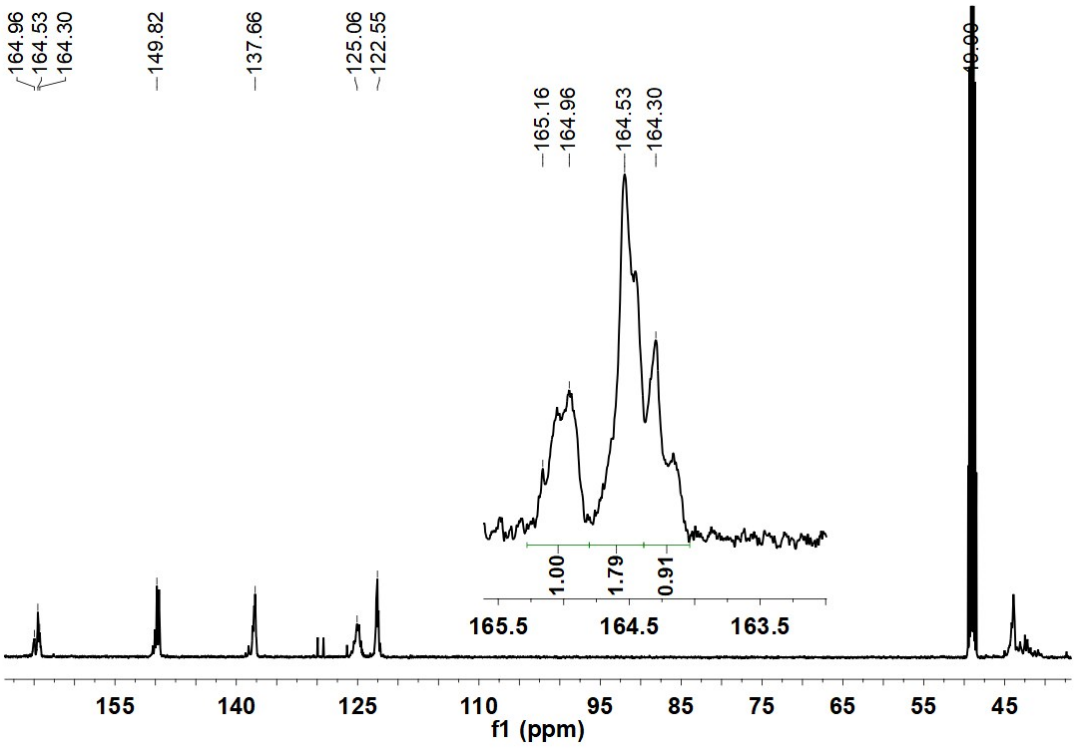

Fig. S17. ^{13}C NMR spectrum (CD_3OD, 125 MHz) of atactic P2VP produced by **2a**/$[Ph_3C][B(C_6F_5)_4]$ in toluene. (mm = 27%)

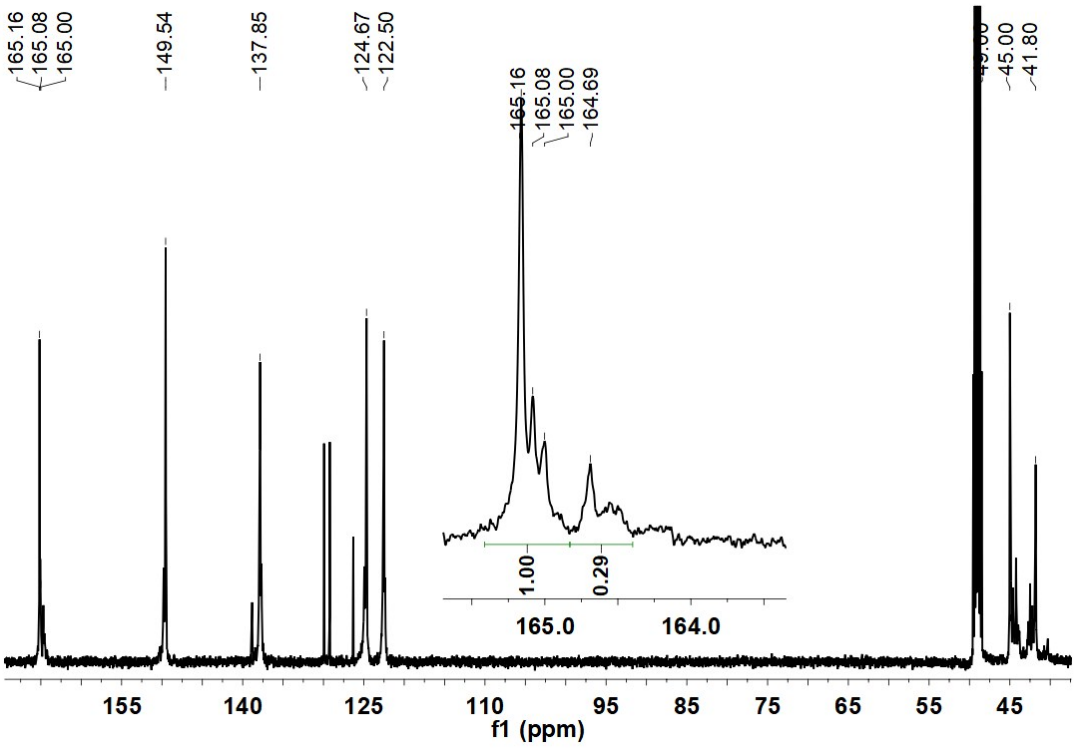

Fig. S18. ^{13}C NMR spectrum (CD_3OD, 125 MHz) of isotactic-rich P2VP produced by $Y(CH_2SiMe_3)_3(THF)_2$/ $[Ph_3C][B(C_6F_5)_4]$ (1 eq.) in toluene. (mm = 78%)

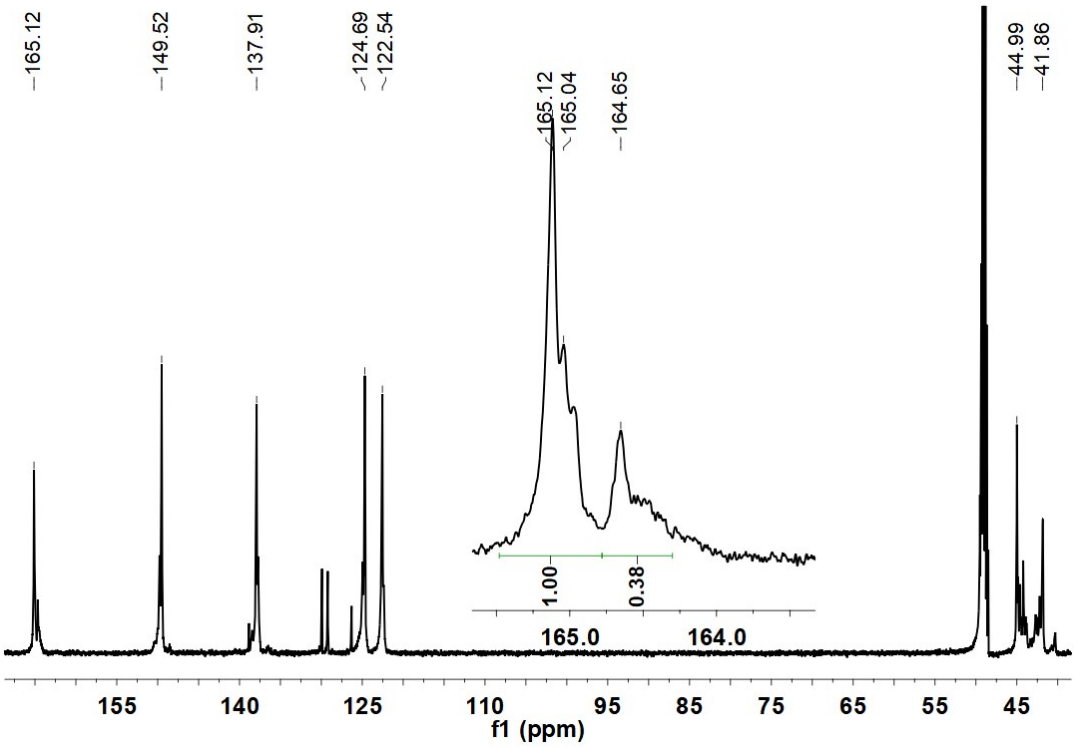

Fig. S19. ^{13}C NMR spectrum (CD_3OD, 125 MHz) of isotactic-rich P2VP produced by $Y(CH_2SiMe_3)_3(THF)_2$/$[Ph_3C][B(C_6F_5)_4]$ (2 eq.) in toluene. (mm = 72%)

4. DSC curves of isotactic P2VP

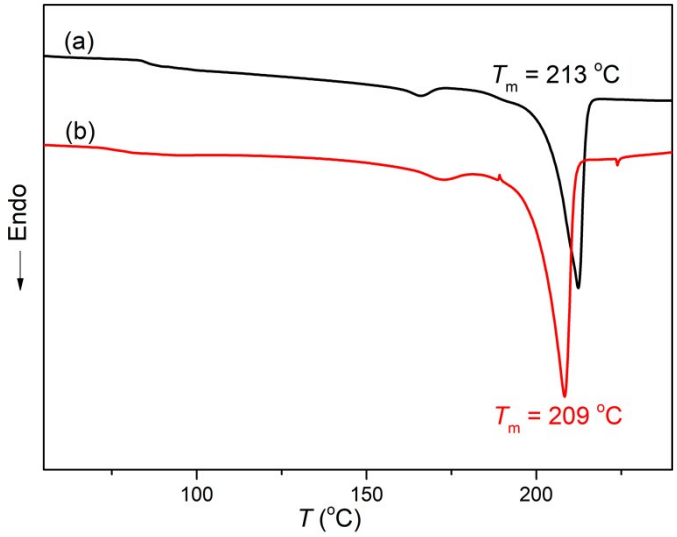

Fig. S20. Differential scanning calorimetry curves of isotactic P2VP produced with (a) **1a**/$[Ph_3C][B(C_6F_5)_4]$ and (b) **1b**/$[Ph_3C][B(C_6F_5)_4]$.

5. MALDI-TOF data and ^{1}H NMR spectrum of 2-VP oligomer

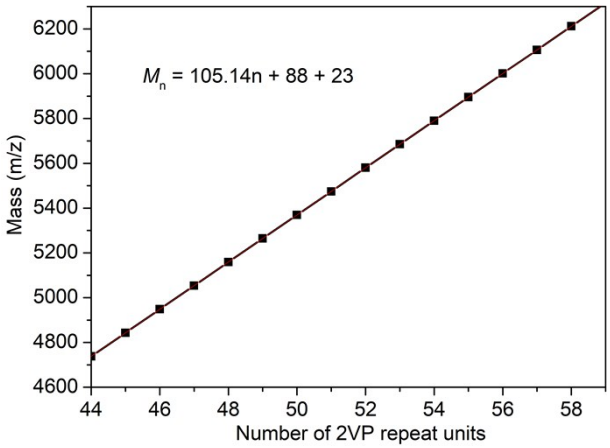

Fig. S21. Plot of molar mass vesus repeat units for a 2-VP oligomer produced with **1a**/[Ph_3C][$B(C_6F_5)_4$].

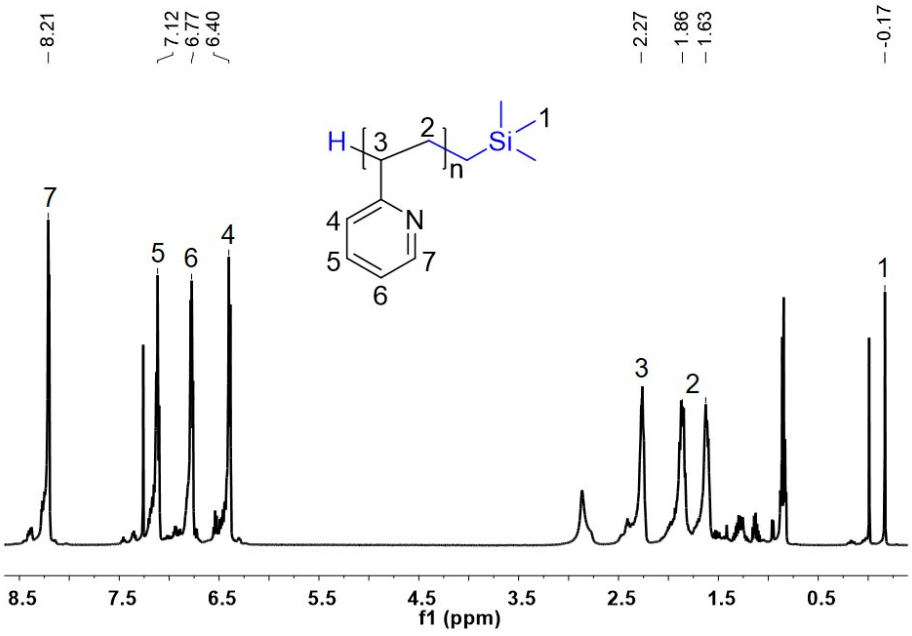

Fig. S22. ^{1}H NMR spectrum (500 MHz, $CDCl_3$) of a 2-VP oligomer produced with **1a**/[Ph_3C][$B(C_6F_5)_4$].

6. Optimizing polymerization time

Table S1. Results of 2-VP polymerization catalyzed by complex **1** with and without $[Ph_3C][B(C_6F_5)_4]$[a)]

Entry	Cat.	Borate	[M]/[Ln]	T (min)	Yield.[b)] (%)	TOF (h^{-1})	$M_{n,exp}$[c)] (kg/mol)	$Đ$[c)]
1	**1a**	-	200	5	98	2352	32.5	1.62
2	**1b**	-	200	5	84	2016	28.6	1.69
3	**1a**	$[Ph_3C][B(C_6F_5)_4]$	200	5	87	2088	20.3	1.11
4	**1b**	$[Ph_3C][B(C_6F_5)_4]$	200	5	99	2376	25.1	1.12

[a)]General conditions: 25 °C, toluene. (2 mL), Cat.: 10 μmol, $[Ph_3C][B(C_6F_5)_4]$: 10 μmol; [b)]Yield determined by gravimetry; [c)]The molecular weight (M_n) and $Đ$ were determined by gel permeation chromatography (GPC) in THF relative to PS.

7. Representative GPC traces of resulting P2VP

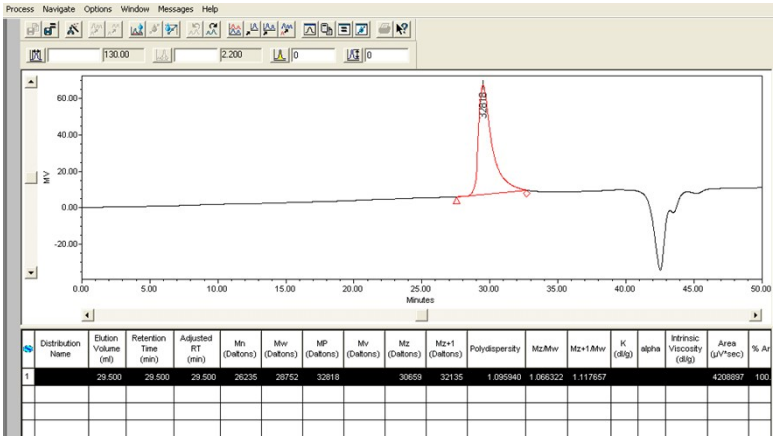

Fig. S23. GPC trace of resulting P2VP produced by **1a**/$[Ph_3C][B(C_6F_5)_4]$ in toluene. (Table 1 entry 5)

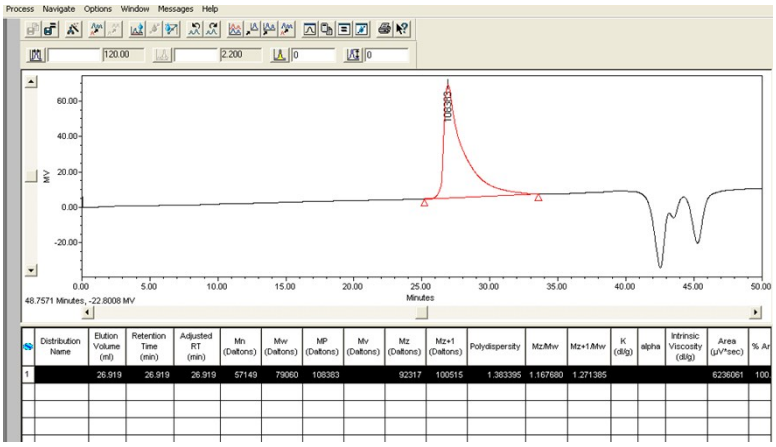

Fig. S24. GPC trace of resulting P2VP produced by **1a**/$[Ph_3C][B(C_6F_5)_4]$ in toluene. (Table 1 entry 9, [2-VP]/**1a** = 500)

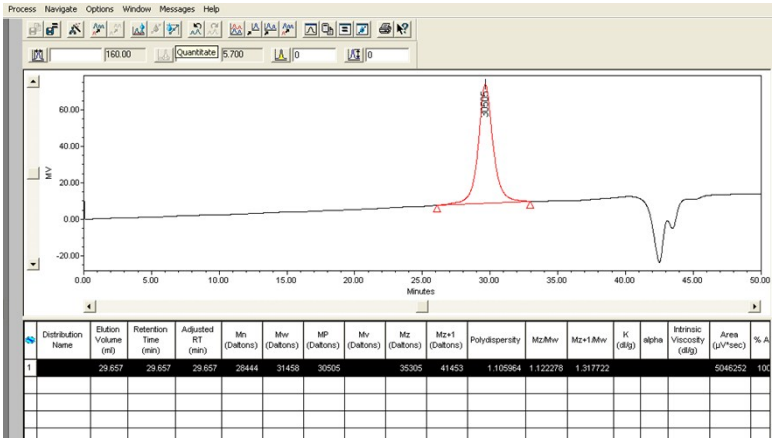

Fig. S25. GPC trace of resulting P2VP produced by **1a**/$[Ph_3C][B(C_6F_5)_4]$ in PhCl. (Table 1 entry 10)

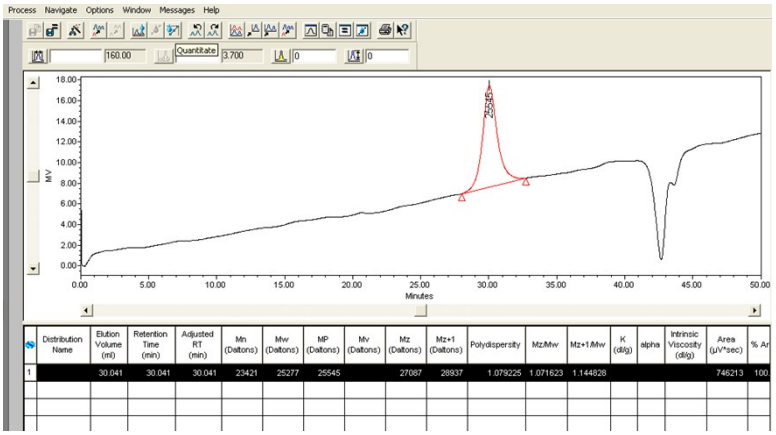

Fig. S26. GPC trace of resulting P2VP produced by **1b**/$[PhNHMe_2][B(C_6F_5)_4]$ in PhCl. (Table 1 entry 14)

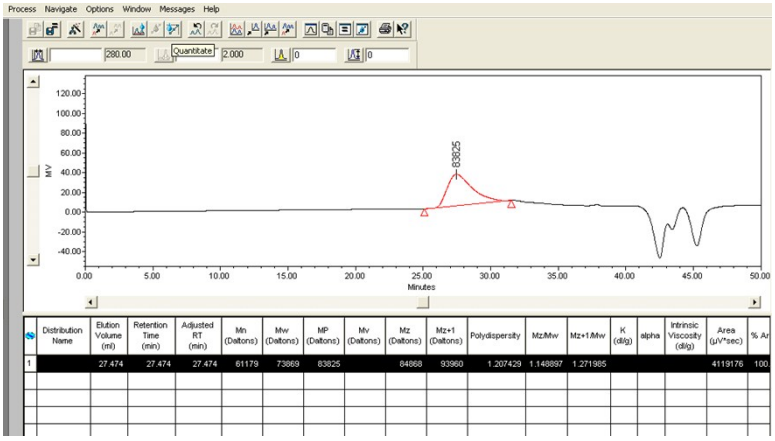

Fig. S27. GPC trace of resulting P2VP produced by $Y(CH_2SiMe_3)_3(THF)_2$/$[Ph_3C][B(C_6F_5)_4]$ (2 eq.) in toluene. (Table 1 entry 16)

8. References

1 (a) T.-Q. Xu, G.-W. Yang and X.-B. Lu, *ACS Catal.*, 2016, **6**, 4907-4913; (b) P. Hubert, A. Soum and M. Fontanille, *Macromol.* Chem. *Phys.,* 1995, **196**, 1023-1030; (c) D. K. Dimov and T. E. Hogen-Esch, *Macromolecules,* 1995, **28**, 7394−7400; (d) M. Brigodiot, H. Cheradame, M. Fontanille and J. P. Vairon, *Polymer,* 1976, **17***,* 254-256.